arXiv:hep-ph/0211238v1 15 Nov 2002

SAGA–HE–195
KYUSHU–HET–62
November 14, 2002

CP Violation in the Higgs Sector and Phase Transition in the MSSM

Koichi FUNAKUBO[a,1], Shuichiro TAO[b,2] and Fumihiko TOYODA[c,3]

[a)] *Department of Physics, Saga University, Saga 840-8502 Japan*

[b)] *Department of Physics, Kyushu University, Fukuoka 812-8581 Japan*

[c)] *Kyushu School of Engineering, Kinki University, Iizuka 820-8555 Japan*

Abstract

We investigate the electroweak phase transition in the presence of a large CP violation in the squark sector of the MSSM. When the CP violation is large, scalar-pseudoscalar mixing of the Higgs bosons occurs and a large CP violation in the Higgs sector is induced. It, however, weakens first-order phase transition before the mixing reaches the maximal. Even when the CP violation in the squark sector is not so large that the phase transition is strongly first order, the phase difference between the broken and symmetric phase regions grows to $\mathcal{O}(1)$, which leads to successful baryogenesis, when the charged Higgs bosons is light.

---

[1] E-mail: funakubo@cc.saga-u.ac.jp
[2] E-mail: tao@higgs.phys.kyushu-u.ac.jp
[3] E-mail: ftoyoda@fuk.kindai.ac.jp

1 Introduction

The baryon asymmetry of the universe (BAU) is one of the most obvious facts, which has been a longstanding problem in astrophysics[1]. To explain the light-element abundances within the framework of the standard big-bang nucleosynthesis, it is required that [2]

$$\frac{n_B}{s} = (0.21 - 0.90) \times 10^{-10}. \tag{1}$$

It is well known that in order to obtain this asymmetry starting from a baryon-symmetric state, three requirements must be satisfied: baryon number violation, C and CP violation, and departure from equilibrium[3]. In general, electroweak theories satisfy baryon number violation through chiral anomaly and have a possibility to generate the BAU[4]. In the minimal standard model(MSM), the main source of CP violation comes from the phase $\delta_{\rm KM}$ in the Cabibbo-Kobayashi-Maskawa (CKM) quark mixing matrix. Although this phase is able to account for the experimentally observed CP violation in the neutral K-mesons and, as recently measured, in the B_d system, it has been shown that it is not possible to generate sufficient BAU through $\delta_{\rm KM}$. Furthermore, the strength of the phase transition is so weak in the MSM with the Higgs scalar heavier than 115GeV[5, 6] that the universe is approximately in equilibrium, when baryon number changing process is in effective.

In the context of supersymmetric (SUSY) extension of the MSM, it has been pointed out that in the presence of a light stop the electroweak phase transition (EWPT) can be strong enough for baryogenesis to take place[7]. Moreover, SUSY models contain many complex parameters as new CP-violating sources in addition to $\delta_{\rm KM}$; the Higgs bilinear term, μ and soft SUSY breaking terms (gaugino masses and scalar trilinear couplings) [8]. Besides these complex parameters, the relative phase of the expectation values of the two Higgs doublets θ might be induced by radiative and finite-temperature effects, although it vanishes at the tree level. Without any complex parameter, the phase θ could be induced by loop effects of SUSY particles. At zero temperature, this idea of spontaneous CP violation was studied in the minimal supersymmetric standard model (MSSM) and it is pointed out that there inevitably appears a pseudoscalar boson as light as several GeV[9]. The same mechanism at finite temperatures was suggested in Ref. [10] and extensively studied by some of us[11]. They found that θ could be large only in the transient region between the symmetric and broken phase regions, with a pseudoscalar Higgs whose mass satisfies $m_A \lesssim 85$GeV. This mechanism was appealing in that such a large θ can produce sufficient BAU and it does not induce a large θ in our vacuum, which is consistent with the bound from neutron electric dipole moment (nEDM). This scenario, however, is now excluded since the mass of the pseudoscalar must satisfy $m_A \geq 90.1$GeV[2].

Nonzero θ is also induced from complex parameters in the MSSM. But magnitude of explicit CP violation is constrained by nEDM measurements. For example, the physical CP phase relevant to the EDM must be as small as $\mathcal{O}(10^{-3})$ when masses of the SUSY particles are weak scale, or they are heavier than 1TeV when the phases are $\mathcal{O}(1)$[8, 12]. Recently it was observed that the spectrum and interactions of the neutral Higgs bosons are affected by a large explicit CP violation in the third generation of squarks sector, which is not restricted by the nEDM constraints[13]. The authors found that when the imaginary part of the product of μ and the Higgs-squark trilinear coupling is large, the lightest Higgs boson H_1, which is composed of the scalar and pseudoscalar Higgs fields, becomes much lighter than the present bound 115GeV, but is hard to be observed, since its couplings to the gauge boson and to the bottom quarks is very small.

One may think that this CP violation can generate sufficient BAU in the MSSM for parameter sets allowed by experiments. Our purpose is to investigate the effects of the explicit CP violation on the EWPT in the MSSM and to evaluate the magnitude of CP violation relevant to electroweak baryogenesis, which should be measured at the transition temperature. The organization of the paper is as follows. In Section 2, we formulate the effective potential of the Higgs fields including the one-loop corrections from the gauge bosons and the third generation of quarks and squarks, both at zero and finite temperatures. The masses of the three neutral Higgs bosons and the charged Higgs boson are defined as the derivatives of the effective potential at the zero-temperature vacuum. The mass formulas are almost the same as those in Ref. [13] except for inclusion of the gauge boson contributions. In Section 3, we study the EWPT for parameter sets, which are consistent with the mass bounds on the neutral lightest and charged Higgs bosons, in the absence of the explicit CP violation. Next we introduce the phase of the trilinear coupling, examine how the strength of the phase transition changes, and evaluate the magnitude of the CP violation relevant to electroweak baryogenesis. Section 4 is devoted to concluding remarks. We summarize the formulas for the Higgs masses in Appendices.

2 Effective potential of the MSSM

We consider the MSSM that has the following superpotential,

$$\mathcal{W} = \epsilon_{ij}\left(f^{(d)}_{AB} H^i_d Q^j_A D_B - f^{(u)}_{AB} H^i_u U_B - \mu H^i_d H^j_u \right). \tag{2}$$

Besides supersymmetric lagrangian, the low-energy MSSM contains the soft-SUSY-breaking terms

$$\begin{aligned} \mathcal{L}_{\text{soft}} = & - \tilde{m}_1^2 \Phi_d^\dagger \Phi_d - \tilde{m}_2^2 \Phi_u^\dagger \Phi_u + \epsilon_{ij}\left(\tilde{m}_3^2 \Phi_d^i \Phi_u^j + \text{h.c.} \right) \\ & - m^2_{\tilde{q}AB} \tilde{q}^\dagger_{AL} \tilde{q}_{BL} - m^2_{\tilde{d}AB} \tilde{d}^\dagger_{AR} \tilde{d}_{BR} - m^2_{\tilde{u}AB} \tilde{u}^\dagger_{AR} \tilde{u}_{BR} \\ & - \epsilon_{ij}\left[\left(f^{(d)} A^{(d)} \right)_{AB} \Phi^i_d \tilde{q}^j_{AL} \tilde{d}^*_{BR} - \left(f^{(u)} A^{(u)} \right)_{AB} \Phi^i_u \tilde{q}^j_{AL} \tilde{u}^*_{BR} + \text{h.c.} \right]. \end{aligned} \tag{3}$$

We calculate the effective potential of the Higgs fields by taking into account the one-loop contributions from the gauge bosons and the third generation of quarks and squarks. We consider the gauginos to be heavy enough to decouple so that the most dangerous contribution to nEDM from the gluino is negligible. The correction from the leptons, the other quark and squarks can be neglected because of their small Yukawa couplings to the Higgs fields. Now the effective potential at zero temperature is given by

$$V_{\text{eff}}(\Phi_d, \Phi_u; T=0) = V_0(\Phi_d, \Phi_u) + \Delta_0 V(\Phi_d, \Phi_u), \tag{4}$$

where $V_0(\Phi_d, \Phi_u)$ is the tree-level potential

$$V_0 = m_1^2 \Phi_d^\dagger \Phi_d + m_2^2 \Phi_u^\dagger \Phi_u - \left(m_3^2 \epsilon_{ij} \Phi^i_d \Phi^j_u + \text{h.c.} \right) + \frac{g_2^2 + g_1^2}{8} \left(\Phi_d^\dagger \Phi_d - \Phi_u^\dagger \Phi_u \right)^2 + \frac{g_2^2}{2} \left| \Phi_d^\dagger \Phi_u \right|^2, \tag{5}$$

and $\Delta_0 V(\Phi_d, \Phi_u)$ is the one-loop correction written as

$$\begin{aligned}\Delta_0 V \;&\equiv\; \frac{N_C}{32\pi^2}\sum_{q=t,b}\left[\sum_{j=1,2}\left(\bar{m}^2_{\tilde{q}_j}\right)^2\left(\log\frac{\bar{m}^2_{\tilde{q}_j}}{M^2}-\frac{3}{2}\right)-2\left(\bar{m}^2_q\right)^2\left(\log\frac{\bar{m}^2_q}{M^2}-\frac{3}{2}\right)\right] \\ &\quad +\frac{3}{64\pi^2}\left[\left(\bar{m}^2_Z\right)^2\left(\log\frac{\bar{m}^2_Z}{M^2}-\frac{3}{2}\right)+2\left(\bar{m}^2_W\right)^2\left(\log\frac{\bar{m}^2_W}{M^2}-\frac{3}{2}\right)\right]. \qquad (6)\end{aligned}$$

Here $\bar{m}^2_q$, $\bar{m}^2_{\tilde{t}_j}$, $\bar{m}^2_{\tilde{b}_j}$ $\bar{m}^2_Z$ and $\bar{m}^2_W$ are field-dependent masses defined by (19), (20), (21), (23) and (24), respectively M denotes the renormalization scale, which we choose such that the loop corrections vanish at the vacuum. The expression (6) is the same as the one-loop correction in [13], except for our inclusion of the gauge-boson contributions, which strengthen the first-order EWPT.

It is well known that the masses of the Higgs bosons receive large corrections from the loops of the top quark and squarks[14]. Here, the masses of the Higgs bosons are defined by the second derivative of the effective potential at the vacuum. To evaluate them, we parameterize the Higgs fields by the vacuum (v_d, v_u, θ) and fluctuation around it as

$$\Phi_d = \begin{pmatrix} \frac{1}{\sqrt{2}}(v_d + h_d + i a_d) \\ \phi_d^- \end{pmatrix}, \quad \Phi_u = e^{i\theta}\begin{pmatrix} \phi_u^+ \\ \frac{1}{\sqrt{2}}(v_u + h_u + i a_u) \end{pmatrix}. \qquad (7)$$

In the following, we represent the quantities evaluated at the vacuum by $\langle\cdot\cdot\rangle$, that is, evaluated with all the fluctuations being set to zero. Requiring that the first derivatives of the effective potential with respect to the neutral Higgs fields evaluated at the vacuum vanish, that is,

$$\left\langle\frac{\partial V_{\rm eff}}{\partial h_d}\right\rangle = \left\langle\frac{\partial V_{\rm eff}}{\partial h_d}\right\rangle = 0, \qquad \left\langle\frac{\partial V_{\rm eff}}{\partial a_d}\right\rangle = \left\langle\frac{\partial V_{\rm eff}}{\partial a_d}\right\rangle = 0, \qquad (8)$$

we can express m_1^2 and m_2^2 in (5), in terms of $\mathrm{Re}(m_3^2 e^{i\theta})$, $\tan\beta = v_u/v_d$ and the particle masses from the first equation, and $\mathrm{Im}(m_3^2 e^{i\theta})$ in terms of the particle masses from the second equation. Now the mass-squared matrix of the neutral Higgs scalars is expressed as

$$\begin{pmatrix} \mathcal{M}_S^2 & \mathcal{M}_{SP}^2 \\ (\mathcal{M}_{SP}^2)^T & \mathcal{M}_P^2 \end{pmatrix}, \qquad (9)$$

where

$$\begin{aligned}
\left(\mathcal{M}_S^2\right)_{11} &= \left\langle\frac{\partial^2 V_{\rm eff}}{\partial h_d^2}\right\rangle, \quad \left(\mathcal{M}_S^2\right)_{22} = \left\langle\frac{\partial^2 V_{\rm eff}}{\partial h_u^2}\right\rangle, \quad \left(\mathcal{M}_S^2\right)_{12} = \left(\mathcal{M}_S^2\right)_{21} = \left\langle\frac{\partial^2 V_{\rm eff}}{\partial h_d \partial h_u}\right\rangle, \\
\left(\mathcal{M}_P^2\right)_{11} &= \left\langle\frac{\partial^2 V_{\rm eff}}{\partial a_d^2}\right\rangle, \quad \left(\mathcal{M}_P^2\right)_{22} = \left\langle\frac{\partial^2 V_{\rm eff}}{\partial a_u^2}\right\rangle, \quad \left(\mathcal{M}_P^2\right)_{12} = \left(\mathcal{M}_S^2\right)_{21} = \left\langle\frac{\partial^2 V_{\rm eff}}{\partial a_d \partial a_u}\right\rangle, \\
\left(\mathcal{M}_{SP}^2\right)_{11} &= \left\langle\frac{\partial^2 V_{\rm eff}}{\partial h_d \partial a_d}\right\rangle, \quad \left(\mathcal{M}_{SP}^2\right)_{12} = \left\langle\frac{\partial^2 V_{\rm eff}}{\partial h_d \partial a_u}\right\rangle, \\
\left(\mathcal{M}_{SP}^2\right)_{21} &= \left\langle\frac{\partial^2 V_{\rm eff}}{\partial a_d \partial h_u}\right\rangle, \quad \left(\mathcal{M}_{SP}^2\right)_{22} = \left\langle\frac{\partial^2 V_{\rm eff}}{\partial h_u \partial a_u}\right\rangle, \qquad (10)
\end{aligned}$$

where each component is given in Appendix B. One can find that the pseudoscalar elements are factorized as

$$\mathcal{M}_P^2 = \left(\mathcal{M}_P^2\right)_{12} \begin{pmatrix} \tan\beta & 1 \\ 1 & \cot\beta \end{pmatrix}, \tag{11}$$

so that, the unphysical Goldstone mode G^0 can be extracted by

$$\begin{pmatrix} a_d \\ a_u \end{pmatrix} = \begin{pmatrix} \cos\beta & \sin\beta \\ -\sin\beta & \cos\beta \end{pmatrix} \begin{pmatrix} G^0 \\ a \end{pmatrix}. \tag{12}$$

Hence, the mass-squared eigenvalues of the neutral Higgs bosons are the eigenvalues of the matrix

$$\mathcal{M}_0^2 \equiv \begin{pmatrix} (\mathcal{M}_S^2)_{11} & (\mathcal{M}_S^2)_{12} & \frac{1}{\cos\beta}(\mathcal{M}_{SP}^2)_{12} \\ (\mathcal{M}_S^2)_{12} & (\mathcal{M}_S^2)_{22} & \frac{1}{\sin\beta}(\mathcal{M}_{SP}^2)_{21} \\ \frac{1}{\cos\beta}(\mathcal{M}_{SP}^2)_{12} & \frac{1}{\sin\beta}(\mathcal{M}_{SP}^2)_{21} & \frac{1}{\sin\beta\cos\beta}(\mathcal{M}_P^2)_{12} \end{pmatrix}. \tag{13}$$

In the presence of the CP violation which induces the scalar-pseudoscalar mixing, the pseudoscalar is no longer a mass eigenstate. In what follows, we use the mass of the charged Higgs boson as an input parameter, instead of the pseudoscalar. The mass matrix of the charged Higgs scalar has the form of

$$\mathcal{M}_\pm^2 = \left\langle \frac{\partial^2 V_{\text{eff}}}{\partial\phi_d^+ \partial\phi_u^-} \right\rangle \begin{pmatrix} \tan\beta & 1 \\ 1 & \cot\beta \end{pmatrix}.$$

Similarly, we can extract the Goldstone mode so that he mass of the charged scalar is given by

$$m_{H^\pm}^2 = \frac{1}{\sin\beta\cos\beta}\left(\mathcal{M}_\pm^2\right)_{12}. \tag{14}$$

The detailed form of the mass is given in Appendix C, by which one can express $\text{Re}(m_3^2 e^{i\theta})$ in terms of $m_{H^\pm}$.

The effective potential at finite temperature contains temperature-dependent corrections;

$$V_{\text{eff}}(\Phi_d, \Phi_u; T) = V_{\text{eff}}(\Phi_d, \Phi_u; T=0) + \Delta_T V(\Phi_d, \Phi_u; T), \tag{15}$$

where

$$\begin{aligned} \Delta_T V = \quad & \frac{T^4}{2\pi^2}\left[6 I_B\left(\frac{\bar{m}_W^2(\Phi)}{T^2}\right) + 3 I_B\left(\frac{\bar{m}_Z^2(\Phi)}{T^2}\right)\right] \\ & + 6\cdot\frac{T^4}{2\pi^2}\sum_{q=t,b}\left[-2 I_F\left(\frac{\bar{m}_q^2(\Phi)}{T^2}\right) + \sum_{j=1,2} I_B\left(\frac{\bar{m}_{\tilde{t}_{q_j}}^2(\Phi)}{T^2}\right)\right]. \end{aligned} \tag{16}$$

Here the functions $I_B(a^2)$ and $I_F(a^2)$ are defined by

$$I_{B,F}(a^2) = \int_0^\infty dx\, x^2 \log\left(1 \mp e^{-\sqrt{x^2+a^2}}\right). \tag{17}$$

The function $I(a^2)$ yields a^3-term with negative coefficient when expanded for $a^2 \ll 1$[15]. This qualitatively explains why the EWPT becomes first order with bosons whose field-dependent mass-squared behave as $\bar{m}^2(v) \sim v^2$ for small v^2. Because of its large Yukawa coupling, a stop with a vanishing soft mass makes the first-order EWPT stronger. In the following, we will not use the high-temperature expansion ($m^2/T^2 \ll 1$), but numerically calculate the integrations to study the EWPT quantitatively.

An important constraint on the finite-temperature effective potential comes from the requirement that the sphaleron process decouples immediately after the EWPT, in order for baryon asymmetry produced at the EWPT not to be washed out. If we denote the minimum of the effective potential as (v_d, v_u, θ), the first-order EWPT is characterized by the degenerate minima at the transition temperature T_C; $(v_C \cos\beta_C, v_C \sin\beta_C, \theta_C)$ in the broken phase region and $(0, 0, \theta_0)$ in the symmetric phase region. The sphaleron decoupling condition is now written as[16]

$$\frac{v_C}{T_C} > 1. \tag{18}$$

The difference between θ_C and θ_0 is crucial to determine total amount of baryon asymmetry produced at the EWPT. The profile of the bubble wall created at the first-order EWPT is derived from the equation of motion for the gauge-Higgs system with the effective potential at T_C[17]. Then the boundary conditions for the Higgs fields are provided by $(v_C \cos\beta_C, v_C \sin\beta_C, \theta_C)$ and $(0, 0, \theta_0)$. Since the bubble wall profile smoothly interpolates between the degenerate minima, the phase θ varies from θ_0 to θ_C at the phase boundary. If there is no local minimum of the effective potential at T_C which leads to the transitional CP violation[11], we expect that the phase monotonously varies so that the baryon number generated is characterized by $\theta_C - \theta_0$. Once we choose the phase convention such that $\theta = 0$ at the zero-temperature vacuum, both θ_C and θ_0 are definitely calculated from the effective potential in the presence of the explicit CP violation in the squark sector. As seen from (8), $\mathrm{Im}(m_3^2)$ becomes nonzero and $\theta_0 = -\delta$ with $\delta \equiv \mathrm{Arg}(m_3^2)$[4]. Then $\theta_C + \delta$ is another important quantity we must evaluate. As shown in various works, when $\theta_C + \delta$ is $\mathcal{O}(1)$, sufficient BAU is generated by the charge transport mechanism[18].

3 Numerical results

There are many parameters in the model, some of which can be fixed by requiring the vacuum at zero temperature to be the prescribed one characterized by $v_0 = 246\mathrm{GeV}$, $\tan\beta$ and θ. In practice, we determine m_1^2 and m_2^2 by use of the tadpole condition (8). $\mathrm{Re}(m_3^2 e^{i\theta})$ can also be determined, once the charged Higgs mass $m_{H^\pm}$ is given by (44). In order to evaluate the right-hand-sides of these equations, one must prepare μ and the parameters in the squark sector; soft masses $m_{\tilde{q}}$, $m_{\tilde{t}_R}$ and $m_{\tilde{b}_R}$, trilinear couplings A_t and A_b. Since the CP symmetry is violated by nonzero $\mathrm{Im}(\mu A_t)$ and $\mathrm{Im}(\mu A_b)$, we take μ to be real and regard the phases of the A-parameters as inputs. The EWPT is strongly first order when the soft mass of squark is very small, as noted in the last section. One usually choose $m_{\tilde{t}} \simeq 0$ and $m_{\tilde{q}} = \mathcal{O}(100)$GeV to avoid too large corrections to the ρ-parameter. For definiteness, we take $m_{\tilde{t}_R} = 10$GeV, $m_{\tilde{b}_R} = 100$GeV, and several values of $m_{\tilde{q}}$ larger than 1TeV. As seen from the scalar-pseudoscalar mixing elements of the mass-squared matrix (13), the CP violation induced in the Higgs sector is enhanced for a larger $\mathrm{Im}(\mu A_t)$. In the following, we take large values for μ and $|A_t|$, but to avoid a color-and-charge-breaking vacuum, we keep $\mu \cot\beta = A \equiv |A_t| = |A_b|$[5]. Thus all the input parameters are $\tan\beta$, μ, $m_{H^\pm}$, $m_{\tilde{q}}$ and $\delta_A = \mathrm{Arg}A_t = \mathrm{Arg}A_b$.

---

[4] In the second paper of [17], the relation $\theta_0 = -\delta$ is proved by use of the kink ansatz for the wall profile. One can show that this relation generally holds, by use of the asymptotic expansion of the wall profile in the symmetric phase.

First of all, we turn off CP violation and calculate masses of the neutral Higgs bosons for various $\tan\beta$, $m_{H^\pm}$, μ and $m_{\tilde{q}}$. Among parameter sets consistent with the present bounds on the lightest Higgs boson mass m_{H_1}, we pick up several ones, for which the EWPT is investigated. We numerically calculate the effective potential (15), and search for the minimum by use of the downhill simplex algorithm. We define T_C as the temperature at which this minimum degenerates with the symmetric phase, and evaluate v_C, $\tan\beta_C$ and θ_C. Next we gradually increase δ_A and examine T_C, v_C and $\theta_C + \delta$.

Before showing the numerical results, we roughly describe how the spectrum, CP violation and the strength of the EWPT depend on the parameters. If we increase $m_{H^\pm}$, which implies larger $\mathrm{Re}(m_3^2)$, the masses of the neutral Higgs boson grow and scalar-pseudoscalar mixing decreases, since the diagonal elements of (13) increases. Then, as is well known, the EWPT becomes stronger for larger $m_{H^\pm}$. If we decrease $\tan\beta$, which implies larger top Yukawa coupling y_t and larger A for a fixed μ, the EWPT becomes stronger and Higgs-mixing is enhanced. As for the effects of δ_A, we expect that the strength of the first-order EWPT will be weakened. This is because nonzero δ_A modifies v-dependence of the mass-squared of the lighter stop, which is roughly proportional to v^2 when $m_{\tilde{t}_R} = 0$ and $\delta_A = 0$, as seen from (26).

Now we present numerical results. In the absence of CP violation, the bounds on the mass of the lightest neutral Higgs excludes the most portion of theoretically allowed region[2]. For small $\tan\beta$, the lower bound is the same as the MSM, $m_h \geq 115$GeV. For $\tan\beta$ between 8 and 40, the lightest Higgs boson can be as light as 92GeV. Very large $\tan\beta$-region is excluded by the fact that CDF at Fermilab have not observed $b\bar{b}$-pair from the lightest Higgs boson. As for the charged scalar, the bounds are satisfied with $m_{H^\pm} \geq 90$GeV for $\tan\beta = 1 - 50$. First of all, we turned off the CP violation and calculated the masses of the Higgs bosons for $\tan\beta = 5$, 10, 20 and 30. For each $\tan\beta$, we studied the EWPT at several points $(\mu, m_{\tilde{q}})$ which are allowed by the Higgs mass bounds. An example of contour plots of the lightest Higgs mass in $(m_{H^\pm}, m_{\tilde{q}})$-plane is shown in Fig. 1. There is no parameter set with $\tan\beta = 5$ for which the EWPT is strongly first order satisfying (18). For $\tan\beta = 10$, 20, we found several parameter sets with small $m_{\tilde{q}}$ for which the EWPT is strongly first order. The lightest Higgs boson mass is smaller than about 110GeV for such parameter sets.

Next, introducing CP violating phase δ_A, we studied the strength of the EWPT and the CP violation relevant to electroweak baryogenesis at several parameter sets for which the Higgs mass bounds are satisfied and the EWPT is strongly first order in the absence of the CP violation. In our convention, $\delta_A \simeq \pi$ is disfavored by the $b \to s\gamma$ constraint[19].

---

[5] In practice, we also studied the case with $\mu \cot\beta \neq A$, but the results are not so altered as long as the squarks do not have nonzero expectation value.

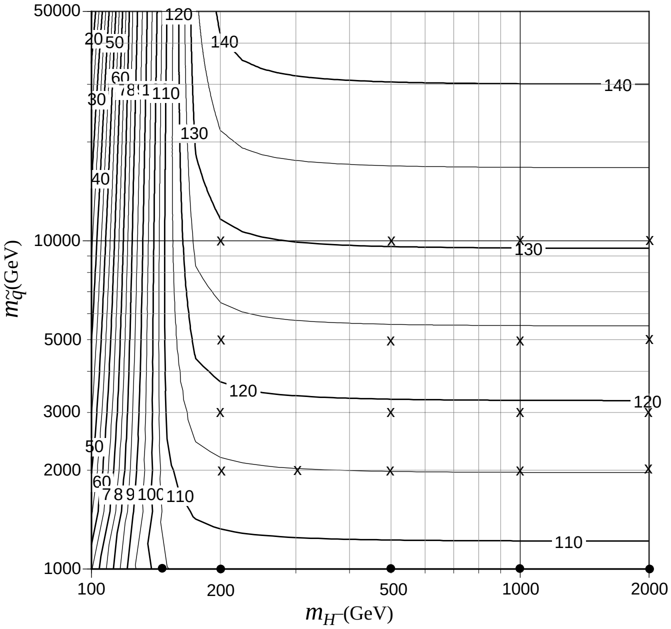

Figure 1: The lightest Higgs mass for $\tan\beta = 10$ and $\mu = 1500$GeV. The dot stands for parameter set for which the EWPT is strongly first order, and the cross for that not satisfying (18).

For example, the results are shown in Fig. 2 for the point in Fig. 1 with $m_{H^\pm} = 150$GeV and $m_{\tilde q} = 1$TeV. Although we do not show the mass of the second-lightest Higgs boson,

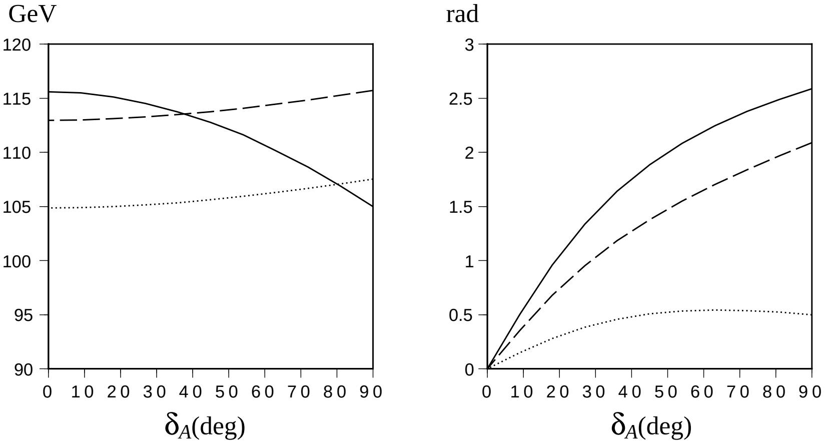

Figure 2: In the left-hand figure, the δ_A-dependences of v_C (solid curve), T_C (dashed curve) and the lightest Higgs mass m_{H_1} (dotted curve) are plotted for $\tan\beta = 10$, $\mu = 1500$GeV, $m_{H^\pm} = 150$GeV and $m_{\tilde q} = 1$TeV. In the left-hand figure, the dashed curve stands for $\delta \equiv \mathrm{Arg}(m_3^2)$, the dotted curve for θ_C and the solid curve for $\theta_C + \delta$ for the same parameter set.

the mixing in the Higgs bosons becomes maximal for $\delta_A > 90$deg. The strength of the

EWPT becomes too weak to satisfy the sphaleron decoupling condition (18) for $\delta_A \gtrsim$ 40deg. The magnitude of CP phase relevant to baryogenesis is sufficiently large for $\delta_A \gtrsim$ 10deg, in spite of small Higgs mixing. For a larger charged Higgs mass, the EWPT becomes stronger, while the Higgs mixing becomes smaller, as expected. The results for $m_{H^\pm} = 200$GeV are shown in Fig. 3. The strongly first-order EWPT persists for $\delta_A \lesssim$ 55deg, while the magnitude of $\theta_C + \delta$ decreases. We also examined the EWPT and the CP phase for larger $m_{H^\pm}$'s and found that the strongly first order EWPT persists for larger δ_A, but $|\theta_C + \delta|$ becomes very small. For example, the maximal value of $|\theta_C + \delta|$ is about 0.02 for $m_{H^\pm} = 1$TeV and 0.005 for $m_{H^\pm} = 2$TeV.

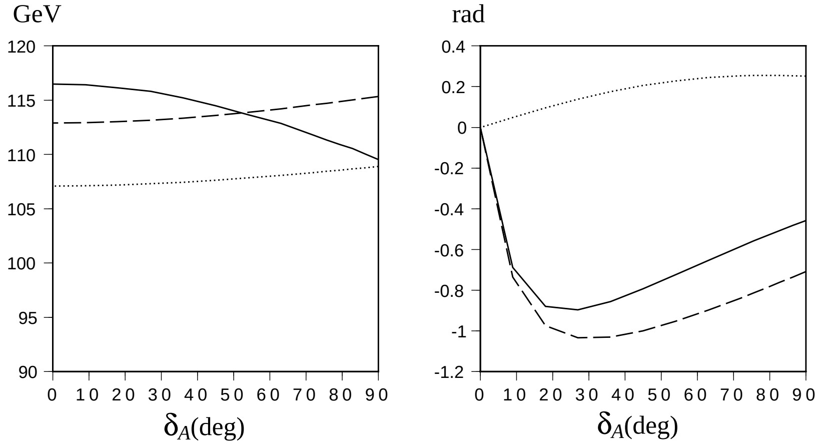

Figure 3: The same as Fig. 2 but with $m_{H^\pm} = 200$GeV.

For larger μ, the effect of δ_A is expected to become stronger, that is, the EWPT is weakened for smaller δ_A. The results for $\mu = 2500$GeV and $m_{\tilde{q}} = 1100$GeV are depicted in Fig. 4. The strongly first-order EWPT persists for $\delta_A \lesssim$ 30degree, while $|\theta_C + \delta|$ is $\mathcal{O}(1)$ for $\delta_A \simeq$ 20degree. If we increase $m_{H^\pm}$, the EWPT gets stronger so that (18) is satisfied up to larger δ_A, but the magnitude of CP violation $|\theta_C + \delta|$ decreases, as the

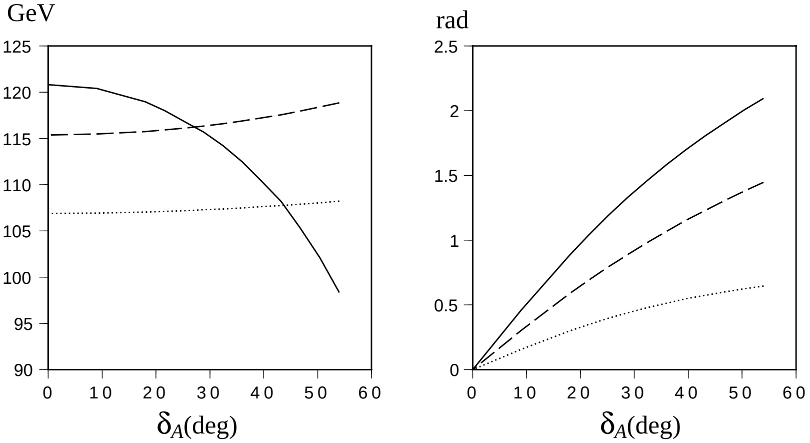

Figure 4: The same as Fig. 3 but with $\mu = 2500$GeV and $m_{\tilde{q}} = 1100$GeV.

case with smaller μ. As an example of a larger $\tan\beta$, we show the results for $\tan\beta = 20$, $\mu = 2500$GeV and $m_{\tilde{q}} = 1220$GeV in Fig. 5. As noted above, a larger $\tan\beta$ implies a smaller top Yukawa coupling, so that the effect of CP violation in the stop sector decreases. In fact, Fig. 5 shows that the strongly first-order EWPT persists for a larger δ_A and $|\theta_C + \delta|$ is smaller than than the case with $\tan\beta = 10$ (Fig. 4). We also explored other parameter sets with the same $\tan\beta$ and observed the same tendency as the case with $\tan\beta = 10$.

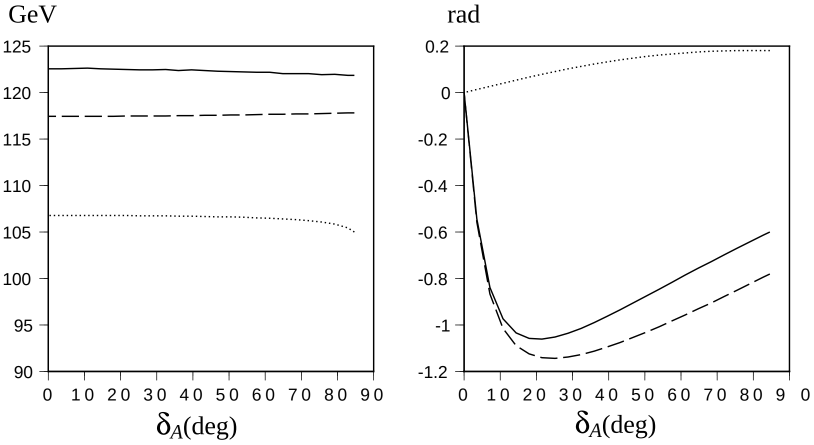

Figure 5: The same as Fig. 3 but with $\tan\beta = 20$, $\mu = 2500$GeV and $m_{\tilde{q}} = 1220$GeV.

4 Conclusion

We have studied the EWPT and CP violation in the Higgs sector of the MSSM. For parameter sets consistent with the present bounds on the masses of neutral and charged Higgs bosons, we found strongly first-order EWPT when the lighter stop mass is less than that of the top quark and the lightest Higgs mass is less than about 110GeV for $8 \lesssim \tan\beta \lesssim 30$, in the absence of CP violation. These results without CP violation are not new. Since the transitional CP violation cannot occur for parameter sets consistent with the updated Higgs boson mass bounds, viable CP violations for electroweak baryogenesis are among those in the complex parameters in the model. The relative phase between μ and gaugino soft mass is essential for the scenario in which the charginos and neutralinos play the role of charge carriers, while the phase is strongly constrained by the neutron EDM bound. If the masses of charginos and neutralinos are found to be as heavy as 1TeV, they cannot participate the baryogenesis, since they can hardly be excited at the EWPT temperature. Another source of CP violation is the relative phase between μ and the squark-Higgs trilinear coupling A. In particular, that phase in the third generation is free from the nEDM constraint, and is expected to play an important role in baryogenesis. Further, it was pointed out that the explicit CP violation in the stop sector can make the scalar-pseudoscalar mixing in the Higgs bosons very large so that the Higgs boson lighter than the present bound is allowed because of their couplings to the gauge bosons and b-quarks[13]. We investigated how this phase affects the EWPT. We found that for a larger phase, the scalar-pseudoscalar mixing increases, but the first-order EWPT becomes weaker. The EWPT cannot continue to be strong enough for successful electroweak baryogenesis before the mixing reaches the maximal. Hence the Higgs scalar lighter than the present bound, which is allowed with a large explicit CP violation, is not consistent with the strongly first-order EWPT which is essential for electroweak baryogenesis. We, however, found that the phase relevant for the baryogenesis can be sufficiently large for the parameter sets consistent with the present mass bounds of the Higgs bosons. Since baryon asymmetry produced by the electroweak baryogenesis depends on the phase difference of the Higgs sector between the broken and symmetric phase regions, which are separated by the bubble wall created at the first-order EWPT. In our phase convention, the phase is $\theta_C + \delta$. The phase can be $\mathcal{O}(1)$ for $m_{H_1} \lesssim 110\text{GeV}$, $m_{H^\pm} \lesssim 200\text{GeV}$ and $8 \lesssim \tan\beta \lesssim 20$, and decreases for a larger $m_{H^\pm}$.

The calculations here are done at the one-loop level. At finite temperatures, the naive loop expansion is not always reliable, and the resummed perturbation with temperature-corrected masses will improve the approximation. In particular, the infrared behavior of the Higgs scalar loop must be treated carefully. This is the reason why the results based on perturbation in the MSM was modified by the improved perturbation or nonperturbative lattice calculation. As for the MSSM, the EWPT is mainly controlled by the stop loops, and the one-loop results in Ref.[20] are consistent with the results obtained by improved perturbation[21] and nonperturbative lattice calculation[22, 23], for the parameters with small $m_{\tilde{t}_R}$, μ and A. We expect that the results in this work will not be altered by such improvements.

The parameter region of the MSSM allowed by the Higgs mass bounds is now much narrower than that allowed theoretically. Within that region, strongly first-order EWPT is possible only for $m_{\tilde{t}_1} \lesssim m_t$ and $m_{H_1} \lesssim 110\text{GeV}$, which corresponds to $8 \lesssim \tan\beta \lesssim 30$. The explicit CP violation in the stop sector can induce large CP phase in the Higgs sector which is relevant to electroweak baryogenesis. Whether this scenario works or not depends on the spectrum of the lightest Higgs boson, charged Higgs boson and the lighter stop. The masses of these particles will be clarified in the near future by LHC. If the lightest Higgs boson is heavier than 110GeV, the EWPT will be too weak to make the sphaleron process out of equilibrium. Even if the EWPT is strongly first order, the model with heavy charged Higgs boson and large μ requires another source of CP violation than that in the Higgs sector for successful electroweak baryogenesis. It might be the relative phases of μ and the gaugino masses, which are constrained by nEDM experiments. For these phase to work, the masses of the charginos and neutralinos should be as light as the weak scale, and it will also be checked in the near future.

Acknowledgements

The authors gratefully thank to A. Kakuto and S. Otsuki for valueble discussions. This work is supported in part by a Grand-in-Aid for Scientific Research No. 13135222 from the Japan Society for the Promotion of Science.

A Field-dependent masses

In this section, we summarize the field-dependent masses of the quarks and squarks of the third generation, and that of the gauge bosons, which appear in the definition of the effective potential (4). These are functions of the neutral components of the Higgs fields, while the charged components are needed to calculate the mass of the charged Higgs boson. The masses of the quark of the third generation are given by

$$\bar{m}^2_{t,b} = \frac{1}{2}\left[|y_t|^2\,\Phi_u^\dagger\Phi_u + |y_b|^2\,\Phi_d^\dagger\Phi_d \pm \sqrt{(|y_t|^2\,\Phi_u^\dagger\Phi_u - |y_b|^2\,\Phi_d^\dagger\Phi_d)^2 + 4\left|\Phi_d^\dagger\Phi_u\right|^2}\,\right]. \tag{19}$$

Similarly, the top and bottom squark masses are

$$\begin{aligned}\bar{m}^2_{\tilde{t}_{1,2}} = \frac{1}{2}\Bigg\{ & m^2_{\tilde{q}} + m^2_{\tilde{t}_R} + 2\,|y_t|^2\,\Phi_u^\dagger\Phi_u + \frac{g_2^2+g_1^2}{4}\left(\Phi_d^\dagger\Phi_d - \Phi_u^\dagger\Phi_u\right) \\ & \pm\sqrt{\left[m^2_{\tilde{q}} - m^2_{\tilde{t}_R} + x_t\left(\Phi_d^\dagger\Phi_d - \Phi_u^\dagger\Phi_u\right)\right]^2 + 2\,|y_t|^2\,|\mu(v_d+h_d+ia_d) - A_t^* e^{-i\theta}(v_u+h_u-ia_u)|^2}\,\Bigg\},\end{aligned} \tag{20}$$

$$\begin{aligned}\bar{m}^2_{\tilde{b}_{1,2}} = \frac{1}{2}\Bigg\{ & m^2_{\tilde{q}} + m^2_{\tilde{b}_R} + 2\,|y_b|^2\,\Phi_d^\dagger\Phi_d - \frac{g_2^2+g_1^2}{4}\left(\Phi_d^\dagger\Phi_d - \Phi_u^\dagger\Phi_u\right) \\ & \pm\sqrt{\left[m^2_{\tilde{q}} - m^2_{\tilde{b}_R} + x_b\left(\Phi_d^\dagger\Phi_d - \Phi_u^\dagger\Phi_u\right)\right]^2 + 2\,|y_b|^2\,|\mu e^{i\theta}(v_u+h_u+ia_u) - A_b^*(v_d+h_d-ia_d)|^2}\,\Bigg\},\end{aligned} \tag{21}$$

where

$$x_t \equiv \frac{1}{4}\left(g_2^2 - \frac{5}{3}g_1^2\right), \quad x_b \equiv -\frac{1}{4}\left(g_2^2 - \frac{1}{3}g_1^2\right). \tag{22}$$

The gauge bosons masses are

$$\begin{aligned}\bar{m}^2_Z &= \frac{1}{4}(g_2^2+g_1^2)\left[(v_d+h_d)^2 + a_d^2 + (v_u+h_u)^2 + a_u^2\right] && (23)\\ \bar{m}^2_W &= \frac{1}{4}g_2^2\left[(v_d+h_d)^2 + a_d^2 + (v_u+h_u)^2\right]. && (24)\end{aligned}$$

The masses evaluated at the zero-temperature vacuum are given as follows:

$$\begin{aligned} m_t^2 &= \left\langle \bar{m}_t^2 \right\rangle = \frac{1}{2}\,|y_t|^2\,v_u^2, \qquad m_b^2 = \left\langle \bar{m}_b^2 \right\rangle = \frac{1}{2}\,|y_b|^2\,v_d^2, && (25)\\ m^2_{\tilde{t}_{1,2}} &= \left\langle \bar{m}^2_{\tilde{t}_{1,2}} \right\rangle \\ &= \frac{m^2_{\tilde{q}} + m^2_{\tilde{t}_R}}{2} + m_t^2 + \frac{1}{4}m_Z^2\cos(2\beta) \\ &\qquad \pm\frac{1}{2}\sqrt{\left[m^2_{\tilde{q}} - m^2_{\tilde{t}_R} + \frac{x_t}{2}v_0^2\cos(2\beta)\right]^2 + 4m_t^2\,|\mu\cot\beta - A_t^* e^{-i\theta}|^2} && (26)\\ m^2_{\tilde{b}_{1,2}} &= \left\langle \bar{m}^2_{\tilde{b}_{1,2}} \right\rangle \end{aligned}$$

$$
\begin{aligned}
&= \frac{m_{\tilde{q}}^2 + m_{\tilde{b}_R}^2}{2} + m_b^2 - \frac{1}{4} m_Z^2 \cos(2\beta) \\
&\quad \pm \frac{1}{2} \sqrt{\left[m_{\tilde{q}}^2 - m_{\tilde{b}_R}^2 + \frac{x_b}{2} v_0^2 \cos(2\beta) \right]^2 + 4 m_b^2 \left| \mu e^{i\theta} \tan\beta - A_b^* \right|^2}, \qquad (27) \\
m_Z^2 &= \frac{1}{4}(g_2^2 + g_1^2) v_0^2, \qquad m_W^2 = \frac{1}{4} g_2^2 v_0^2, \qquad (28)
\end{aligned}
$$

where $v_0^2 \equiv v_d^2 + v_u^2$, $\tan\beta = v_u / v_d$.

B Mass matrix of the neutral Higgs boson

The calculation of the elements of the mass matrix is presented in Ref.[13]. We included the gauge-boson contributions to their calculation, so that we record their explicit forms. For later convenience, we introduce the following quantities:

$$
M_t^2 = m_{\tilde{q}}^2 - m_{\tilde{t}_R}^2 + \frac{x_t}{2} v_0^2 \cos(2\beta), \qquad M_b^2 = m_{\tilde{q}}^2 - m_{\tilde{b}_R}^2 + \frac{x_b}{2} v_0^2 \cos(2\beta), \qquad (29)
$$

$$
\Delta m_{\tilde{q}}^2 = m_{\tilde{q}_1}^2 - m_{\tilde{q}_2}^2, \qquad (q = t, b) \qquad (30)
$$

$$
R_q = \mathrm{Re}\left(\mu A_q e^{i\theta} \right), \quad I_q = \mathrm{Im}\left(\mu A_q e^{i\theta} \right), \qquad (q = t, b) \qquad (31)
$$

$$
P_t = |\mu|^2 - R_t \tan\beta, \qquad Q_t = |A_t|^2 - R_t \cot\beta, \qquad (32)
$$

$$
P_b = |\mu|^2 - R_b \cot\beta, \qquad Q_b = |A_b|^2 - R_b \tan\beta. \qquad (33)
$$

The elements of the mass matrix in the scalar sector are given by

$$
\begin{aligned}
\left(\mathcal{M}_S^2 \right)_{11} = {} & \mathrm{Re}(m_3^2 e^{i\theta}) \tan\beta + m_Z^2 \cos^2\beta \\
& + \frac{N_C}{16\pi^2} \Bigg\{ \frac{1}{2} m_Z^2 \cos^2\beta \left(\frac{x_t M_t^2 + 2|y_t|^2 P_t}{\Delta m_{\tilde{t}}^2} \log\frac{m_{\tilde{t}_1}^2}{m_{\tilde{t}_2}^2} - \frac{x_b M_b^2 + 2|y_b|^2 Q_b}{\Delta m_{\tilde{b}}^2} \log\frac{m_{\tilde{b}_1}^2}{m_{\tilde{b}_2}^2} \right) \\
& + 2 m_b^2 \left(\frac{x_b M_b^2 + 2|y_b|^2 Q_b}{\Delta m_{\tilde{b}}^2} \log\frac{m_{\tilde{b}_1}^2}{m_{\tilde{b}_2}^2} - 2|y_b|^2 \log\frac{m_b^2}{M^2} \right) \\
& + v_d^2 \left(\frac{g_2^2 + g_1^2}{8} \right)^2 \left(\log\frac{m_{\tilde{t}_1}^2}{M^2} + \log\frac{m_{\tilde{t}_2}^2}{M^2} \right) + v_d^2 \left(|y_b|^2 - \frac{g_2^2 + g_1^2}{8} \right)^2 \left(\log\frac{m_{\tilde{b}_1}^2}{M^2} + \log\frac{m_{\tilde{b}_2}^2}{M^2} \right) \\
& + \frac{x_t^2 v_d^2 + 2|y_t|^2 R_t \tan\beta}{2\Delta m_{\tilde{t}}^2} \left(m_{\tilde{t}_1}^2 \log\frac{m_{\tilde{t}_1}^2}{M^2} - m_{\tilde{t}_2}^2 \log\frac{m_{\tilde{t}_2}^2}{M^2} - \Delta m_{\tilde{t}}^2 \right) \\
& + \frac{x_b^2 v_d^2 + 2|y_b|^2 R_b \tan\beta}{2\Delta m_{\tilde{b}}^2} \left(m_{\tilde{b}_1}^2 \log\frac{m_{\tilde{b}_1}^2}{M^2} - m_{\tilde{b}_2}^2 \log\frac{m_{\tilde{b}_2}^2}{M^2} - \Delta m_{\tilde{b}}^2 \right) \\
& + v_d^2 \frac{(x_t M_t^2 + 2|y_t|^2 P_t)^2}{2(\Delta m_{\tilde{t}}^2)^2} \left(1 - \frac{m_{\tilde{t}_1}^2 + m_{\tilde{t}_2}^2}{2\Delta m_{\tilde{t}}^2} \log\frac{m_{\tilde{t}_1}^2}{m_{\tilde{t}_2}^2} \right) \\
& + v_d^2 \frac{(x_b M_b^2 + 2|y_b|^2 Q_b)^2}{2(\Delta m_{\tilde{b}}^2)^2} \left(1 - \frac{m_{\tilde{b}_1}^2 + m_{\tilde{b}_2}^2}{2\Delta m_{\tilde{b}}^2} \log\frac{m_{\tilde{b}_1}^2}{m_{\tilde{b}_2}^2} \right) \Bigg\} \\
& + \frac{3}{128\pi^2} v_d^2 \left\{ (g_2^2 + g_1^2)^2 \log\frac{m_Z^2}{M^2} + 2 g_2^4 \log\frac{m_W^2}{M^2} \right\}, \qquad (34)
\end{aligned}
$$

$$
\begin{aligned}
\left(\mathcal{M}_S^2\right)_{22} = {} & \mathrm{Re}(m_3^2 e^{i\theta})\cot\beta + m_Z^2 \sin^2\beta \\
& + \frac{N_C}{16\pi^2}\Bigg\{ \frac{1}{2} m_Z^2 \sin^2\beta \left(-\frac{-x_t M_t^2 + 2\left|y_t\right|^2 Q_t}{\Delta m_{\tilde{t}}^2} \log\frac{m_{\tilde{t}_1}^2}{m_{\tilde{t}_2}^2} + \frac{-x_b M_b^2 + 2\left|y_b\right|^2 P_b}{\Delta m_{\tilde{b}}^2} \log\frac{m_{\tilde{b}_1}^2}{m_{\tilde{b}_2}^2} \right) \\
& + 2 m_t^2 \left(\frac{-x_t M_t^2 + 2\left|y_t\right|^2 Q_t}{\Delta m_{\tilde{t}}^2} \log\frac{m_{\tilde{t}_1}^2}{m_{\tilde{t}_2}^2} - 2\left|y_t\right|^2 \log\frac{m_t^2}{M^2} \right) \\
& + v_u^2 \left(\left|y_t\right|^2 - \frac{g_2^2 + g_1^2}{8} \right)^2 \left(\log\frac{m_{\tilde{t}_1}^2}{M^2} + \log\frac{m_{\tilde{t}_2}^2}{M^2} \right) + v_u^2 \left(\frac{g_2^2 + g_1^2}{8} \right)^2 \left(\log\frac{m_{\tilde{b}_1}^2}{M^2} + \log\frac{m_{\tilde{b}_2}^2}{M^2} \right) \\
& + \frac{x_t^2 v_u^2 + 2\left|y_t\right|^2 R_t \cot\beta}{2\Delta m_{\tilde{t}}^2} \left(m_{\tilde{t}_1}^2 \log\frac{m_{\tilde{t}_1}^2}{M^2} - m_{\tilde{t}_2}^2 \log\frac{m_{\tilde{t}_2}^2}{M^2} - \Delta m_{\tilde{t}}^2 \right) \\
& + \frac{x_b^2 v_u^2 + 2\left|y_b\right|^2 R_b \cot\beta}{2\Delta m_{\tilde{b}}^2} \left(m_{\tilde{b}_1}^2 \log\frac{m_{\tilde{b}_1}^2}{M^2} - m_{\tilde{b}_2}^2 \log\frac{m_{\tilde{b}_2}^2}{M^2} - \Delta m_{\tilde{b}}^2 \right) \\
& + v_u^2 \frac{(-x_t M_t^2 + 2\left|y_t\right|^2 Q_t)^2}{2(\Delta m_{\tilde{t}}^2)^2} \left(1 - \frac{m_{\tilde{t}_1}^2 + m_{\tilde{t}_2}^2}{2\Delta m_{\tilde{t}}^2} \log\frac{m_{\tilde{t}_1}^2}{m_{\tilde{t}_2}^2} \right) \\
& + v_u^2 \frac{(-x_b M_b^2 + 2\left|y_b\right|^2 P_b)^2}{2(\Delta m_{\tilde{b}}^2)^2} \left(1 - \frac{m_{\tilde{b}_1}^2 + m_{\tilde{b}_2}^2}{2\Delta m_{\tilde{b}}^2} \log\frac{m_{\tilde{b}_1}^2}{m_{\tilde{b}_2}^2} \right) \Bigg\} \\
& + \frac{3}{128\pi^2} v_u^2 \left\{ (g_2^2 + g_1^2)^2 \log\frac{m_Z^2}{M^2} + 2 g_2^4 \log\frac{m_W^2}{M^2} \right\},
\end{aligned}
\tag{35}
$$

$$
\begin{aligned}
\left(\mathcal{M}_S^2\right)_{12} = {} & -\mathrm{Re}(m_3^2 e^{i\theta}) - m_Z^2 \sin\beta\cos\beta \\
& + \frac{N_C}{16\pi^2}\Bigg\{ \frac{1}{2} m_Z^2 \sin\beta\cos\beta \left(\frac{-x_t M_t^2 + \left|y_t\right|^2 (Q_t - P_t)}{\Delta m_{\tilde{t}}^2} \log\frac{m_{\tilde{t}_1}^2}{m_{\tilde{t}_2}^2} \right. \\
& \qquad\qquad \left. + \frac{x_b M_b^2 + \left|y_b\right|^2 (Q_b - P_b)}{\Delta m_{\tilde{b}}^2} \log\frac{m_{\tilde{b}_1}^2}{m_{\tilde{b}_2}^2} \right) \\
& + m_t^2 \cot\beta \frac{x_t M_t^2 + 2\left|y_t\right|^2 P_t}{\Delta m_{\tilde{t}}^2} \log\frac{m_{\tilde{t}_1}^2}{m_{\tilde{t}_2}^2} + m_b^2 \tan\beta \frac{-x_b M_b^2 + 2\left|y_b\right|^2 P_b}{\Delta m_{\tilde{b}}^2} \log\frac{m_{\tilde{b}_1}^2}{m_{\tilde{b}_2}^2} \\
& + \frac{1}{2} m_Z^2 \sin\beta\cos\beta \left[\left(\left|y_t\right|^2 - \frac{g_2^2 + g_1^2}{8} \right) \left(\log\frac{m_{\tilde{t}_1}^2}{M^2} + \log\frac{m_{\tilde{t}_2}^2}{M^2} \right) \right. \\
& \qquad\qquad \left. + \left(\left|y_b\right|^2 - \frac{g_2^2 + g_1^2}{8} \right) \left(\log\frac{m_{\tilde{b}_1}^2}{M^2} + \log\frac{m_{\tilde{b}_2}^2}{M^2} \right) \right] \\
& - \frac{x_t^2 v_d v_u + 2\left|y_t\right|^2 R_t}{2\Delta m_{\tilde{t}}^2} \left(m_{\tilde{t}_1}^2 \log\frac{m_{\tilde{t}_1}^2}{M^2} - m_{\tilde{t}_2}^2 \log\frac{m_{\tilde{t}_2}^2}{M^2} - \Delta m_{\tilde{t}}^2 \right) \\
& - \frac{x_b^2 v_d v_u + 2\left|y_b\right|^2 R_b}{2\Delta m_{\tilde{b}}^2} \left(m_{\tilde{b}_1}^2 \log\frac{m_{\tilde{b}_1}^2}{M^2} - m_{\tilde{b}_2}^2 \log\frac{m_{\tilde{b}_2}^2}{M^2} - \Delta m_{\tilde{b}}^2 \right) \\
& + v_d v_u \frac{(x_t M_t^2 + 2\left|y_t\right|^2 P_t)(-x_t M_t^2 + 2\left|y_t\right|^2 Q_t)}{2(\Delta m_{\tilde{t}}^2)^2} \left(1 - \frac{m_{\tilde{t}_1}^2 + m_{\tilde{t}_2}^2}{2\Delta m_{\tilde{t}}^2} \log\frac{m_{\tilde{t}_1}^2}{m_{\tilde{t}_2}^2} \right)
\end{aligned}
$$

$$
\begin{aligned}
&+v_d v_u \frac{(x_b M_b^2 + 2\left|y_b\right|^2 Q_b)(-x_b M_b^2 + 2\left|y_b\right|^2 P_b)}{2(\Delta m_{\tilde{b}}^2)^2}\left(1 - \frac{m_{\tilde{b}_1}^2 + m_{\tilde{b}_2}^2}{2\Delta m_{\tilde{b}}^2}\log\frac{m_{\tilde{b}_1}^2}{m_{\tilde{b}_2}^2}\right)\Bigg\} \\
&+\frac{3}{128\pi^2} v_d v_u \left\{(g_2^2+g_1^2)^2\log\frac{m_Z^2}{M^2} + 2g_2^4\log\frac{m_W^2}{M^2}\right\}. \qquad (36)
\end{aligned}
$$

The matrix elements in the pseudoscalar sector are

$$
\left(\mathcal{M}_P^2\right)_{11} = \left(\mathcal{M}_P^2\right)_{12}\tan\beta, \qquad (37)
$$

$$
\left(\mathcal{M}_P^2\right)_{22} = \left(\mathcal{M}_P^2\right)_{12}\cot\beta, \qquad (38)
$$

$$
\begin{aligned}
\left(\mathcal{M}_P^2\right)_{12} = \mathrm{Re}(m_3^2 e^{i\theta}) + \frac{N_C}{16\pi^2}\Bigg\{ &\frac{\left|y_t\right|^2}{\Delta m_{\tilde{t}}^2}\Bigg[R_t\left(m_{\tilde{t}_1}^2\log\frac{m_{\tilde{t}_1}^2}{M^2} - m_{\tilde{t}_2}^2\log\frac{m_{\tilde{t}_2}^2}{M^2} - \Delta m_{\tilde{t}}^2\right) \\
&+\frac{4m_t^2\cot\beta}{\Delta m_{\tilde{t}}^2} I_t^2\left(1 - \frac{m_{\tilde{t}_1}^2 + m_{\tilde{t}_2}^2}{2\Delta m_{\tilde{t}}^2}\log\frac{m_{\tilde{t}_1}^2}{m_{\tilde{t}_2}^2}\right)\Bigg] \\
&+\frac{\left|y_b\right|^2}{\Delta m_{\tilde{b}}^2}\Bigg[R_b\left(m_{\tilde{b}_1}^2\log\frac{m_{\tilde{b}_1}^2}{M^2} - m_{\tilde{b}_2}^2\log\frac{m_{\tilde{b}_2}^2}{M^2} - \Delta m_{\tilde{b}}^2\right) \\
&+\frac{4m_b^2\tan\beta}{\Delta m_{\tilde{b}}^2} I_b^2\left(1 - \frac{m_{\tilde{b}_1}^2 + m_{\tilde{b}_2}^2}{2\Delta m_{\tilde{b}}^2}\log\frac{m_{\tilde{b}_1}^2}{m_{\tilde{b}_2}^2}\right)\Bigg]\Bigg\}. \qquad (39)
\end{aligned}
$$

The scalar-pseudoscalar mixing elements are given by

$$
\left(\mathcal{M}_{SP}^2\right)_{11} = \left(\mathcal{M}_{SP}^2\right)_{12}\tan\beta, \qquad (40)
$$

$$
\left(\mathcal{M}_{SP}^2\right)_{22} = \left(\mathcal{M}_{SP}^2\right)_{21}\cot\beta, \qquad (41)
$$

$$
\begin{aligned}
\left(\mathcal{M}_{SP}^2\right)_{12} = \frac{N_C}{8\pi^2}\Bigg\{ &\frac{m_t^2 I_t\cot^2\beta}{\Delta m_{\tilde{t}}^2}\left[\frac{g_2^2+g_1^2}{8}\log\frac{m_{\tilde{t}_1}^2}{m_{\tilde{t}_2}^2} + \frac{x_t M_t^2 + 2\left|y_t\right|^2 P_t}{\Delta m_{\tilde{t}}^2}\left(1 - \frac{m_{\tilde{t}_1}^2 + m_{\tilde{t}_2}^2}{2\Delta m_{\tilde{t}}^2}\log\frac{m_{\tilde{t}_1}^2}{m_{\tilde{t}_2}^2}\right)\right] \\
&+\frac{m_b^2 I_b}{\Delta m_{\tilde{b}}^2}\left[\left(\left|y_b\right|^2 - \frac{g_2^2+g_1^2}{8}\right)\log\frac{m_{\tilde{b}_1}^2}{m_{\tilde{b}_2}^2} + \frac{x_b M_b^2 + 2\left|y_b\right|^2 Q_b}{\Delta m_{\tilde{b}}^2}\left(1 - \frac{m_{\tilde{b}_1}^2 + m_{\tilde{b}_2}^2}{2\Delta m_{\tilde{b}}^2}\log\frac{m_{\tilde{b}_1}^2}{m_{\tilde{b}_2}^2}\right)\right]\Bigg\}
\end{aligned}
\qquad (42)
$$

$$
\begin{aligned}
\left(\mathcal{M}_{SP}^2\right)_{21} = \frac{N_C}{8\pi^2}\Bigg\{ &\frac{m_t^2 I_t}{\Delta m_{\tilde{t}}^2}\left[\left(\left|y_t\right|^2 - \frac{g_2^2+g_1^2}{8}\right)\log\frac{m_{\tilde{t}_1}^2}{m_{\tilde{t}_2}^2} + \frac{-x_t M_t^2 + 2\left|y_t\right|^2 Q_t}{\Delta m_{\tilde{t}}^2}\left(1 - \frac{m_{\tilde{t}_1}^2 + m_{\tilde{t}_2}^2}{2\Delta m_{\tilde{t}}^2}\log\frac{m_{\tilde{t}_1}^2}{m_{\tilde{t}_2}^2}\right)\right] \\
&+\frac{m_b^2 I_b\tan^2\beta}{\Delta m_{\tilde{b}}^2}\left[\frac{g_2^2+g_1^2}{8}\log\frac{m_{\tilde{b}_1}^2}{m_{\tilde{b}_2}^2} + \frac{-x_b M_b^2 + 2\left|y_b\right|^2 P_b}{\Delta m_{\tilde{b}}^2}\left(1 - \frac{m_{\tilde{b}_1}^2 + m_{\tilde{b}_2}^2}{2\Delta m_{\tilde{b}}^2}\log\frac{m_{\tilde{b}_1}^2}{m_{\tilde{b}_2}^2}\right)\right]\Bigg\},
\end{aligned}
\qquad (43)
$$

which are all composed of the terms proportional to $\mathrm{Im}(\mu A_t)/\Delta m_{\tilde{t}}^2$ or $\mathrm{Im}(\mu A_b)/\Delta m_{\tilde{b}}^2$.

C Charged Higgs mass

The calculation of the charged Higgs mass is a tedious task, and the method is described in Appendix of Ref.[13]. We present the result, which contain the contribution from the gauge bosons:

$$\begin{aligned}
m_{H^\pm}^2 = {} & \frac{1}{\sin\beta\cos\beta}\mathrm{Re}(m_3^2 e^{i\theta}) + m_W^2 \\
& + \frac{N_C}{16\pi^2\sin\beta\cos\beta}\Bigg\{\frac{1}{\Delta m_{\tilde t}^2}\left[\left(\frac{f(m_{\tilde t_1}^2)}{(m_{\tilde t_1}^2 - m_{\tilde b_1}^2)(m_{\tilde t_1}^2 - m_{\tilde b_2}^2)} + |y_t|^2 R_t\right) m_{\tilde t_1}^2 \left(\log\frac{m_{\tilde t_1}^2}{M^2} - 1\right)\right. \\
& \qquad\qquad\qquad\qquad \left. -(\tilde t_1 \to \tilde t_2)\right] \\
& \qquad + \frac{1}{\Delta m_{\tilde b}^2}\left[\left(\frac{f(m_{\tilde b_1}^2)}{(m_{\tilde b_1}^2 - m_{\tilde t_1}^2)(m_{\tilde b_1}^2 - m_{\tilde t_2}^2)} + |y_b|^2 R_b\right) m_{\tilde b_1}^2 \left(\log\frac{m_{\tilde b_1}^2}{M^2} - 1\right) - (\tilde b_1 \to \tilde b_2)\right] \\
& \qquad - \frac{2\,|y_t y_b|\,m_t m_b}{m_t^2 - m_b^2}\left[m_t^2\left(\log\frac{m_t^2}{M^2} - 1\right) - m_b^2\left(\log\frac{m_t^2}{M^2} - 1\right)\right]\Bigg\} \\
& - \frac{3}{16\pi^2}(g_2^2 + g_1^2)\frac{g_2^2}{g_1^2} m_Z^2 \left(\log\frac{m_Z^2}{M^2} - 1\right),
\end{aligned} \tag{44}$$

where

$$\begin{aligned}
& f(m_{\tilde q_k}^2) \\
& \quad = \frac{1}{2}|y_t y_b|^2 v_u v_d \left[2m_{\tilde q_k}^4 - \mathrm{Tr}(\mathcal{M}_{\tilde t}^2 + \mathcal{M}_{\tilde b}^2) m_{\tilde q_k}^2 + \left(\mathcal{M}_{\tilde t}^2\right)_{11}\left(\mathcal{M}_{\tilde b}^2\right)_{11} + \left(\mathcal{M}_{\tilde t}^2\right)_{22}\left(\mathcal{M}_{\tilde b}^2\right)_{22}\right] \\
& \qquad - \frac{1}{4} g_2^2 v_u v_d \left(|y_t|^2 + |y_b|^2 - \frac{g_2^2}{2}\right)(m_{\tilde q_k}^2 - \left(\mathcal{M}_{\tilde t}^2\right)_{22})(m_{\tilde q_k}^2 - \left(\mathcal{M}_{\tilde b}^2\right)_{22}) \\
& \qquad + \frac{1}{2}|\mu|^2 v_u v_d \Bigg[-(|y_t|^2 + |y_b|^2)\left(|y_t|^2 + |y_b|^2 - \frac{g_2^2}{2}\right) m_{\tilde q_k}^2 \\
& \qquad\qquad + |y_t|^2\left(|y_t|^2 - \frac{g_2^2}{2}\right)\left(\mathcal{M}_{\tilde b}^2\right)_{22} + |y_b|^2\left(|y_b|^2 - \frac{g_2^2}{2}\right)\left(\mathcal{M}_{\tilde t}^2\right)_{22} \\
& \qquad\qquad + |y_t y_b|^2\left(|\mu|^2 + 2m_{\tilde q}^2 + 2m_t^2 + 2m_b^2 - m_W^2 - \frac{g_1^2}{12} v_0^2 \cos(2\beta)\right)\Bigg] \\
& \qquad + \frac{1}{2}|y_t A_t|^2 v_u v_d \left(|y_b|^2 - \frac{g_2^2}{2}\right)(m_{\tilde q_k}^2 - \left(\mathcal{M}_{\tilde b}^2\right)_{22}) + \frac{1}{2}|y_b A_b|^2 v_u v_d \left(|y_t|^2 - \frac{g_2^2}{2}\right)(m_{\tilde q_k}^2 - \left(\mathcal{M}_{\tilde t}^2\right)_{22}) \\
& \qquad + \frac{1}{2}|y_t y_b A_t A_b|^2 v_u v_d - |y_t y_b|^2 v_u v_d (R_t R_b + I_t I_b) \\
& \qquad - 2m_t^2 m_b^2\left[\left(|y_b|^2 - \frac{g_2^2}{2}\right) R_t + \left(|y_t|^2 - \frac{g_2^2}{2}\right) R_b\right] \\
& \qquad + \frac{1}{2}|y_t y_b|^2 v_u v_d \mathrm{Re}(A_t A_b^*)\left[2m_{\tilde q_k}^2 - 2m_{\tilde q}^2 - m_W^2 + \frac{g_1^2}{12} v_0^2 \cos(2\beta)\right].
\end{aligned} \tag{45}$$

References

[1] E. D. Kolb and M. S. Turner, *The Early Universe* (Perseus Publishing, 1994).

[2] Particle Data Group, Phys. Rev. **D45** (2002) 010001.

[3] A. D. Sakharov, Pisma Zh. Eksp. Teor. Fiz. **5** (1967) 32; JETP Lett. **5** (1967) 24.

[4] For a review see, A. Cohen, D. Kaplan and A. Nelson, Ann. Rev. Nucl. Part. Sci. **43** (1993) 27.
V. A. Rubakov and M. E. Shaposhnikov, Phys. Usp. **39** (1996) 461.
K. Funakubo, Prog. Theor. Phys. **96** (1996) 475.
A. Riotto and M. Trodden, Ann. Rev. Nucl. Part. Sci. **49** (1999) 35.

[5] A. I. Bochkarev, S. V. Kuzmin and M. E. Shaposhinikov, Phys. Lett. **B244** (1990) 275.

[6] For nonperturbative study on the lattice see the following papers and references therein.
F. Csikor, Z. Fodor and J. Heitger, Phys. Lett. **B441** (1998) 354; Phys. Rev. Lett. **82** (1999) 21.
Y. Aoki, F. Csikor, Z. Fodor and A. Ukawa, Phys. Rev. **D60** (1999) 114511.

[7] A. Brignole, J. R. Espinosa, M. Quiros and F. Zwirner, Phys. Lett. **B324** (1994) 181.
M. Carena, M. Quiros and C. E. M. Wagner, Phys. Lett. **B380** (1996) 81.
D. Delepine, J. M. Gerard, R. G. Filipe and J. Weyers, Phys. Lett. **B386** (1996) 183.
J. M. Cline and G. D. Moore, Phys. Rev. Lett. **81** (1998) 3315.

[8] M. Dugan, B. Grinstein and L. Hall, Nucl. Phys. **B255** (1985) 413.

[9] N.Maekawa, Phys. Lett. **B282** (1992) 387; Nucl. Phys. **B** (Proc. Suppl.) **37A** (1994) 191.

[10] D. Comelli, M. Pietroni and A. Riotto, Nucl. Phys. **B412** (1994) 441.

[11] K. Funakubo, A. Kakuto, S. Otsuki and F. Toyoda, Prog. Theor. Phys. **99** (1998) 1045.
K. Funakubo, S. Otsuki and F. Toyoda, Prog. Theor. Phys. **102** (1999) 389.
M. Laine and K. Rummukainen, Nucl. Phys. **B545** (1999) 141.

[12] Y. Kizukuri and N. Oshimo, Phys. Rev. **D45** (1992) 1806; Phys. Rev. **D46** (1992) 3025.

[13] M. Carena, J. Ellis, A. Pilaftsis and C. E. M. Wagner, Nucl. Phys. **B586** (2000) 92.

[14] Y. Okada, M. Yamaguchi and T. Yanagida, Prog. Theor. Phys. **85** (1991) 1; Phys. Lett. **B262** (1991) 54.
J. Ellis, G. Ridolfi and F. Zwirner, Phys. Lett. **B257** (1991) 83; ibid. **262** (1991) 477.
H. E. Haber and R. Hempfling, Phys. Rev. Lett. **66** (1991) 1815.
J. R. Espinosa and M. Quiros, Phys. Lett. **B266** (1991) 389.
D. M. Pierce, A. Papadopoulos and S. B. Johnson, Phys. Rev. Lett. **68** (1992) 3678.

[15] L. Dolan and R. Jackiw, Phys. Rev. **D9** (1974) 3320.

[16] M. E. Shaposhnikov, JETP Lett. **44** (1986) 465; Nucl. Phys. **287** (1987) 757.

[17] K. Funakubo, A. Kakuto, S. Otsuki and F. Toyoda, Prog. Theor. Phys. **98** (1997) 427.

[18] A. Nelson, D. Kaplan and A. Cohen, Nucl. Phys. **B373** (1992) 453.
K. Funakubo, A. Kakuto, S. Otsuki, K. Takenaga and F. Toyoda, Phys. Rev. **D50**

(1994) 1105.
K. Funakubo, A. Kakuto, S. Otsuki and F. Toyoda, Prog. Theor. Phys. **95** (1996) 929.
M. Joyce, T. Prokepec and N. Turok, Phys. Rev. **D50** (1996) 2930.
M. Aoki, A. Sugamoto and N. Oshimo, Prog. Theor. Phys. **98** (1997) 1325.

[19] T. Goto and Y. Okada, Prog. Theor. Phys. **94** (1995) 407.

[20] K. Funakubo, Prog. Theor. Phys. **101** (1999) 415.

[21] B. de Carlos and J. R. Espinosa, Nucl. Phys. **B503** (1997) 24.

[22] M. Laine and K. Rummukainen, Phys. Rev. Lett. **80** (1998) 5259; Nucl. Phys. **B597** (2001) 23.

[23] F. Csikor, Z. Fodor, P. Hegedus, V. K. Horvath, S. D. Katz, A. Piroth, Phys. Rev. Lett. **85** (2000) 932.

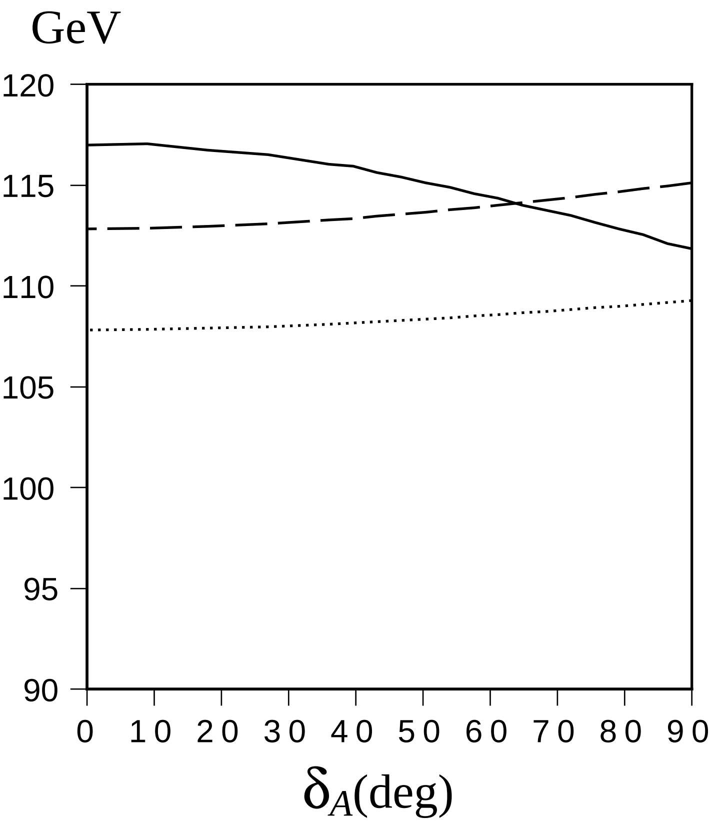
GeV
120
115
110
105
100
95
90
0
10
20
30
40
50
60
70
80
90
δ_A(deg)

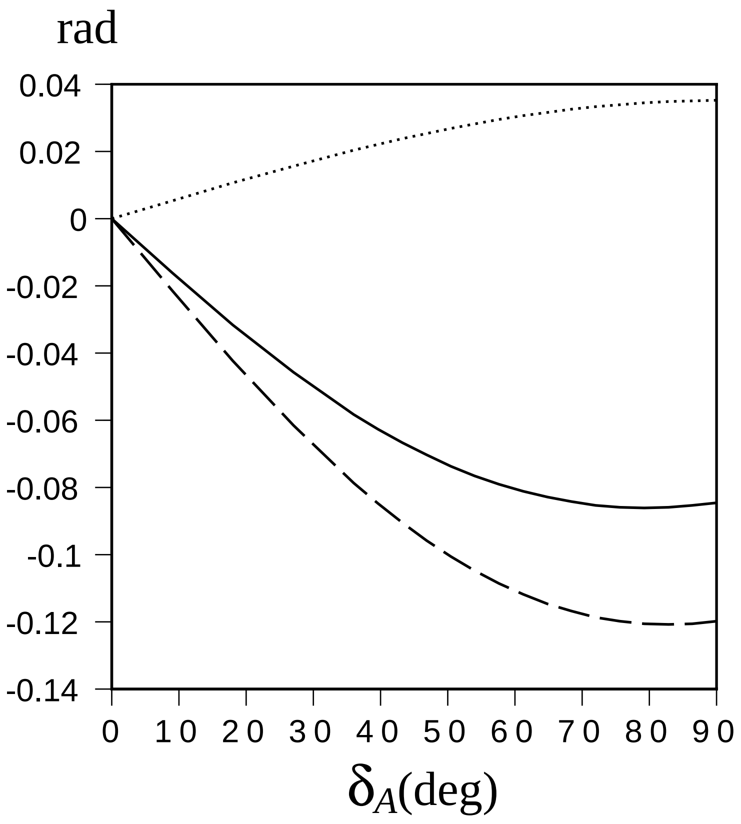
rad
0.04
0.02
0
-0.02
-0.04
-0.06
-0.08
-0.1
-0.12
-0.14
0
10
20
30
40
50
60
70
80
90
δ_A(deg)